Chemical Science

ROYAL SOCIETY OF CHEMISTRY

EDGE ARTICLE

View Article Online
View Journal | View Issue

Cite this: *Chem. Sci.*, 2021, **12**, 11858

All publication charges for this article have been paid for by the Royal Society of Chemistry

Received 30th March 2021
Accepted 4th August 2021

DOI: 10.1039/d1sc01802g

rsc.li/chemical-science

Rigid, biconical hydrogen-bonded dimers that strongly encapsulate cationic guests in solution and the solid state†

Jordan N. Smith, [ab] Courtney Ennis [a] and Nigel T. Lucas *[ab]

The octol of a new rigid, tetraarylene-bridged cavitand was investigated for self-assembly behaviour in solution. ^{1}H and DOSY NMR spectroscopic experiments show that the cavitand readily dimerizes through an unusual seam of interdigitated hydrogen-bonds that is resistant to disruption by polar co-solvents. The well-defined cavity encapsulates small cationic guests, but not their neutral counterparts, restricting the conformation of sequestered tetraethylammonium in solution and the solid state.

Introduction

Confined spaces within self-assembled capsules are distinct from the bulk solvent, sequestering complementary guests[1] or catalysing chemical reactions.[2–4] The volume and morphology of the cavity depends upon the size and shape of the monomers: Rebek's highly-curved arcs homo-dimerize into the spherical tennis balls[5] and softballs[6] (Fig. 1a), whereas the shallow and flexible bowls resorcin[4]arenes and pyrogallol[4]arenes form hexamers[7–14] or dimers[15–22] (Fig. 1b) depending on the solvent and added guests. While hydrogen-bonded assemblies of other molecular bowls are known (trioximes[23] tribenzo-triquinacenes,[24] calix[4]arenes,[25] cyclotriveratrylenes[26] and cyclotricatechylenes[27]), the majority of reported capsules are built upon the readily available resorcin[4]arene scaffold, the intrinsic concave surface and an exoannular array of hydroxyl groups providing the elements for capsular self-assembly. Importantly, the solubility of the macrocycle in polar and non-polar solvents is modulated through the length of the alkyl "feet".[28] The upper-rim of resorcin[4]arenes is readily functionalized, with additional hydrogen-bond donors and acceptors increasing the cavity size and/or strengthening the interaction.[29–33] For example, Rebek's diimide[34] and de Mendoza's benzimidazolone[35] cavitands interact through a seam of 16 bifurcated N–H···O bonds to generate large, cylindrical dimers around complementary guests (Fig. 1c).

We recently reported the synthesis of the novel resorcin[4]arene-derived octamethoxy tetraarylene-bridged cavitand **1a** (Scheme 1), with an enforced, conical cavity that is not subject to the conformational fluxionality experienced by many resorcin[4]arene bowls.[36] As part of further studies into this new class of cavitand, we were interested as to whether its octol, **2a**, would self-assemble into multicomponent aggregates through the four catechol units at the upper-rim (Fig. 1d). The unusual rigidity of the cavitand, combined with the preorganized and inflexible array of exoannular hydroxyl groups, was predicted to give hydrogen-bonded constructs of distinct geometry and high stability. Herein we report the findings of this study, in which **2a** and its undecyl-footed analogue **2b** homo-dimerize through a remarkable circular seam of hydrogen-bonds to give a rigid, biconical capsule with a well-defined cavity (Fig. 1d).

Results and discussion

Cleavage of the eight exoannular methyl ethers of **1a** with BBr_3 in CH_2Cl_2 was facile; however, the product **2a** was insoluble in

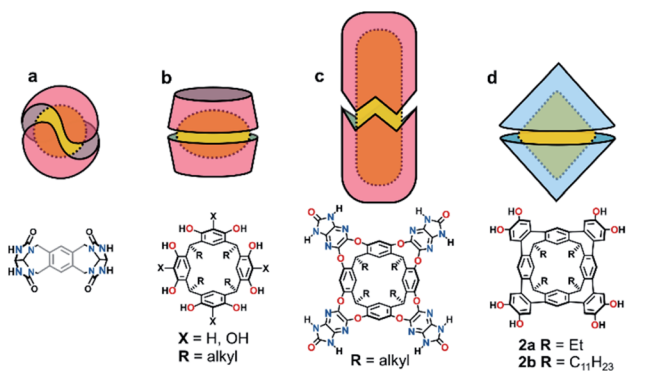

Fig. 1 Cartoon representations of hydrogen-bonded homo-dimeric capsules and chemical diagrams of their monomer units; (a) Rebek's tennis and softballs, (b) resorcin[4]arene dimers, (c) Rebek and de Medoza's cylindrical capsules and (d) the biconical capsules presented in this work.

[a]*Department of Chemistry, University of Otago, Union Place, Dunedin, New Zealand. E-mail: nigel.lucas@otago.ac.nz*

[b]*MacDiarmid Institute for Advanced Materials and Nanotechnology, New Zealand*

† Electronic supplementary information (ESI) available: Synthetic procedures and characterization data of all new compounds; details of solution spectroscopic/crystallographic characterization of dimer and host–guest complexes; details of calculations and electrostatic potential maps. CCDC 2070238. For ESI and crystallographic data in CIF or other electronic format see DOI: 10.1039/d1sc01802g

the non-polar solvents $CHCl_3$ or CH_2Cl_2 (Scheme 1). To improve the solubility in non-polar solvents, we used our recent synthesis of C_{2v}-symmetric resorcin[4]arene derivatives[37] to prepare the undecyl analogue **1b** in eight steps (see ESI†).

Eightfold methyl ether cleavage afforded **2b** in 93% yield, and the macrocycle was found to be soluble in $CHCl_3$, CH_2Cl_2 and acetone. The ^{1}H NMR spectrum of a freshly prepared solution of **2b** in $CDCl_3$ showed three cavitand species in slow exchange on the NMR timescale. Within *ca.* 60 minutes, equilibrium was established showing only a single species of C_{4v}-symmetry, with no further change over days. The nature of the stable species formed from **2b** was investigated by DOSY NMR spectroscopy. Self-assembled aggregates are predicted to diffuse more slowly than their monomers, as shown by the Stokes–Einstein equation in which the diffusion coefficient (D) is inversely proportional to the spherical hydrodynamic radius[38] (see ESI†). Experiments in $CDCl_3$ (Table 1) showed **2b** diffuses more slowly than octamethoxy **1b**—which cannot form multi-component adducts through intermolecular hydrogen-bonding and is an appropriate surrogate for the monomer—but faster than the related resorcin[4]arene hexamers reported by Cohen (2.8×10^{-6} cm^2 s^{-1}; R = $C_{11}H_{23}$).[11,38] The estimated diffusion volume of octol **2b** is 1.7 times that of "monomer" **1b** (see ESI†), consistent with homo-dimerization to **2b**·**2b** driven by mutual hydrogen-bonding interactions at the cavitands' wide rims. An energy-optimised model of the dimer **2′**·**2′** supports this analysis (the prime symbol in **2′**·**2′** denotes calculated structures throughout this text), showing a unidirectional, cyclic seam of eight intermolecular and eight intramolecular hydrogen bonds (Fig. 2). In the ^{1}H NMR spectrum of **2b** ($CDCl_3$, 298 K) a single OH resonance appears at *ca.* 6.89 ppm, its shift largely independent of **2b** concentration across the range 1–14 mM ($\Delta\delta$ = 0.05 ppm; see ESI†). This lone OH signal is consistent with the rapid interconversion between the two equivalent arrangements of hydrogen-bonds on the NMR timescale (Fig. 2).

Further ^{1}H NMR experiments in 20–50% v/v $CHCl_3$/$CDCl_3$ mixtures show solvent is encapsulated by the host, as evidenced by the appearance of $CHCl_3$ resonance at 3.03 ppm ($\Delta\delta$ = −4.23 ppm; see ESI†). Similarly, in 50% v/v C_6D_6/$CDCl_3$ two species are present in a 6 : 1 ratio at equilibrium, corresponding to the complexes **2b**·**2b**⊂**CDCl$_3$** or **2b**·**2b**⊂**C$_6$D$_6$**. The absence of a third species likely excludes the co-capture of two guest molecules.

To probe the stability of the dimer in protic, polar solvents, the diffusion coefficient of **2b**·**2b** in $CDCl_3$ with increasing proportions of CD_3OD (0–800 equiv. per **2b**) was measured by DOSY NMR spectroscopy (see ESI†).[14] D remained consistent with a dimer across the series ($3.4–3.5 \times 10^{-6}$ cm^2 s^{-1}), in mixtures of up to 15% CD_3OD (v/v). This high stability of the complex contrasts with the resorcin[4]arene and pyrogallol[4]arene hexamers studied by Cohen,[14] which show rapid increases in diffusion coefficient upon the addition of small amounts of MeOH. At the limit of solubility (1600 equiv. CD_3OD), a second species appears in slow exchange with the dimer; however, its diffusion coefficient could not be differentiated. Unfortunately, the dimerization constant, K_{dimer}, for **2b** in $CDCl_3$ was not readily established, as concentration titrations of **2b** monitored by UV-visible spectroscopy in $CHCl_3$ or 5% MeOH/$CHCl_3$ showed only a linear response in the Beer–Lambert region (see ESI†), and the weak emission of the cavitand prevented collection of reliable fluorescence spectroscopic titration data. Due to the unique hydrogen-bonding motif, we know of no suitable

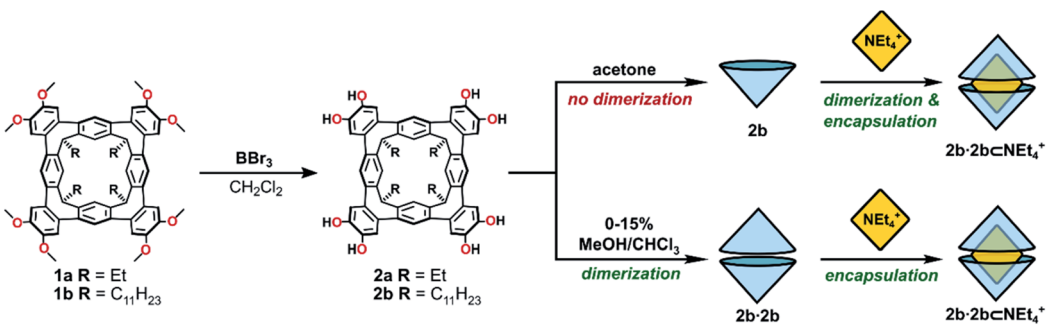

Scheme 1 The synthesis of octol cavitands **2a** and **2b**, and a comparison of self-assembly behaviour of **2b** in acetone or MeOH/$CHCl_3$ mixtures.

Table 1 Experimental diffusion coefficients (D) for cavitands and their complexes measured by DOSY NMR spectroscopy

Entry	Host	Added guest	Solvent	D (10^{-6} cm^2 s^{-1})	Diffusing species
1	**1b**	—	$CDCl_3$	4.10	**1b**
2	**2b**	—	$CDCl_3$	3.45	**2b**·**2b**
3	**2b**	NEt_4Br	$CDCl_3$	3.35	**2b**·**2b**⊂NEt_4^+
4	**1b**	—	$(CD_3)_2CO$	6.95	**1b**
5	**2b**	—	$(CD_3)_2CO$	6.95	**2b**
6	**2b**	NEt_4Br	$(CD_3)_2CO$	5.50	**2b**·**2b**⊂NEt_4^+

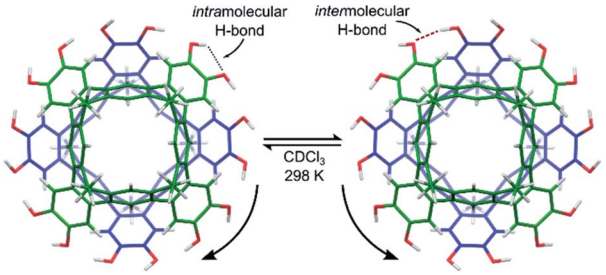

Fig. 2 Energy-optimised model of the dimer complex **2′·2′** (B3LYP-D3/6-31G(d,p) with idealized S_8-symmetry). The fast interconversion between two symmetry-equivalent hydrogen-bonding arrangements is shown.

dimerization constants for direct comparison; however, on the basis of the ^{1}H and DOSY NMR and UV-vis data presented herein, and the high stability of the complex in protic, polar solvents, K_{dimer} for **2b** is likely $>10^6$ M^{-1} and may exceed $>10^9$ M^{-1}. Similar values were reported for a dimeric capsule stabilised by eight hydrogen-bonds.[39]

To assess the guest-binding properties of the cavitand to non-solvent guests, **2b** was combined with NEt_4Br in 1 : 1, 2 : 1 and 4 : 1 ratios in $CDCl_3$ at 298 K and the ^{1}H NMR spectra examined for evidence of encapsulation (Fig. 3). The 1 : 1 mixture showed slow exchange between **2b·2b** and **2b·2b⊂NEt$_4^+$** species, reaching quantitative encapsulation within 60 minutes (Fig. 3b). The free and bound NEt_4^+ species appear as two sets of signals in a 1 : 1 ratio (denoted with blue and yellow circles, respectively; Fig. 3b), as expected for the formation of **2b·2b⊂NEt$_4^+$**. Alkyl signals for the bound cation are dramatically shifted upfield as far as −4.90 ppm ($\Delta\delta = -6.3$ ppm) in response to the shielding influence of the host upon the internalized guest. The high-field ethyl signals of NEt_4^+ appear in two distinct environments as the conformation of the tightly bound guest is restricted within the host, behaviour supported by X-ray crystallography (*vide infra*). When **2b** and NEt_4Br were combined in a 2 : 1 ratio, only the host–guest adduct **2b·2b⊂NEt$_4^+$** is observed (Fig. 3c). DOSY NMR spectroscopy confirmed equal diffusion rates of the host and encapsulated guest at 3.35×10^{-6} cm^2 s^{-1} (Table 1, entry 3), a rate similar to that of the free host **2b·2b**. Increasing the host–guest ratio to 4 : 1 shows complete encapsulation of the guest, with an equimolar amount of residual free dimer host **2b·2b** (Fig. 3d). These data support both the apparent exclusive formation of the homodimer **2b·2b** and quantitative uptake of NEt_4^+ to give **2b·2b⊂NEt$_4^+$**, with both species in slow exchange in $CDCl_3$. The association constant, K_a, for the binding of NEt_4^+ by **2b·2b** is $4.6 \pm 0.3 \times 10^5$ M^{-1} ($\Delta G = -31.9 \pm 1.6$ kJ mol^{-1} in $CHCl_3$, 293 K), as determined by UV-vis titrations[40] of the host with the guest, and assuming a 1 : 1 host : guest binding model on the assumption $K_{dimer} \gg K_a$ (see ESI†).

The coordination of catechol units with halide anions is well known,[41] and similar interactions have been shown to template the formation of resorcin[4]arene and pyrogallol[4]arene capsules.[42] Homo-dimeric resorcin[4]arene-derived capsules formed through intermolecular hydrogen-bonding alone are

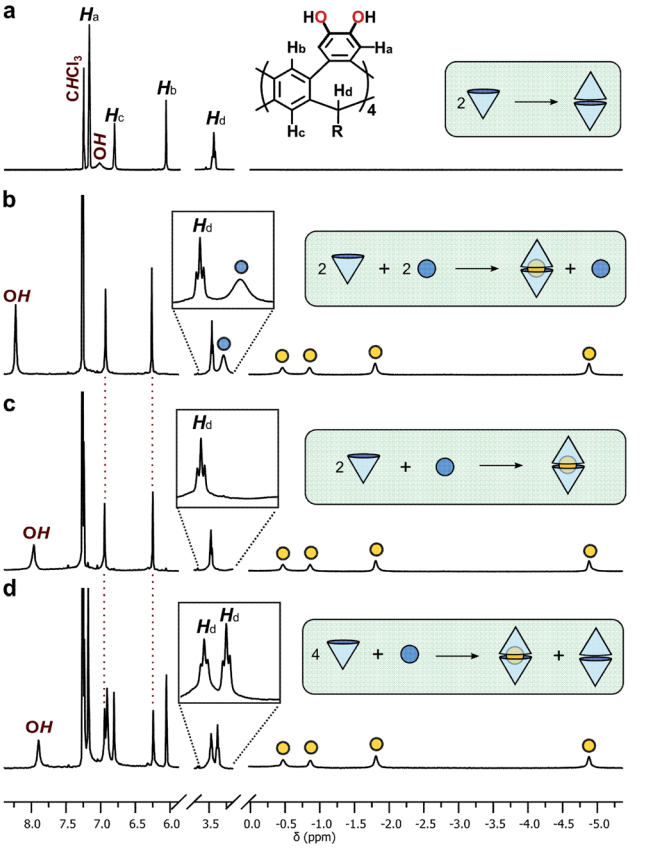

Fig. 3 Truncated ^{1}H NMR spectra ($CDCl_3$, 298 K, 400 MHz) of (a) **2b**, and **2b** and NEt_4Br in (b) 1 : 1, (c) 2 : 1 and (d) 4 : 1 ratios. Bound and free NEt_4^+ cations are represented by yellow and blue circles, respectively. Insets show expansions of the methine proton of the host (H_d) and the methylene protons of the unbound guest.

rare; solvent molecules or the halide counterions of cationic guests are typically incorporated into the hydrogen-bonded network to template the dimerization processes, usually observed only in the solid state.[22] Here, dimerization readily occurs in solution in the absence of templating molecules or anions, and moreover, is unaffected by their presence. Presumably, the low concentration of bromide counterions relative to the complex, combined with the competitive solvent, appear to limit interactions to the periphery of the dimer, causing only a moderate downfield shift in the OH proton resonance that increases with bromide concentration (Fig. 3). The limited role of the bromide ion in bonding at the seam is supported by crystallography (*vide infra*). While beyond the scope of the present study, it is noted that coordinating halide anions at higher concentrations may template different/larger multicomponent adducts and is an interesting avenue for further investigation.

In the bulk polar aprotic solvent d_6-acetone, **2b** failed to dimerize, as shown by the similar diffusion coefficients for **1b** and **2b** (Table 1, entries 4 and 5; Scheme 1; Fig. 4). The addition of excess NEt_4Br to the monomer solution of **2b** saw quantitative formation of the complex **2b·2b⊂NEt$_4^+$**, as evidenced by the shift in OH proton resonance ($\Delta\delta = +1.29$ ppm) consistent with

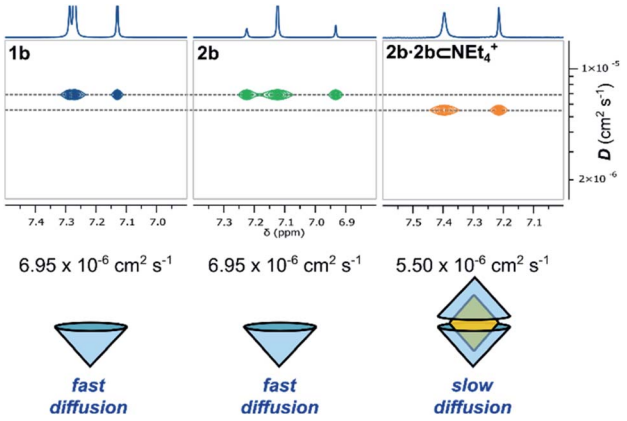

Fig. 4 Truncated ^{1}H and DOSY NMR spectra (d_6-acetone, 298 K, 500 MHz) of **1b**, **2b** and **2b**⊂NEt_4**Br** and their diffusion coefficients.

increased hydrogen-bonding and the reduced diffusion coefficient (Table 1, entry 6). From these data it is clear interactions with the cationic guest play a role in the enthalpic-stabilisation of the dimer in bulk polar media.

The ethyl-footed analogue **2a** and $\mathbf{NEt_4}^+$ (2 : 1) failed to form a soluble **2a**·**2a**⊂$\mathbf{NEt_4}^+$ complex in neat $CDCl_3$; however, following the addition of 20% CD_3OD, the suspension dissolved within 12 hours. ^{1}H NMR analysis again showed complete formation of a 2 : 1 complex in this competitive media (see ESI†). The charged complexes **2a**·**2a**⊂$\mathbf{NEt_4}^+$ and **2b**·**2b**⊂$\mathbf{NEt_4}^+$ observed in solution were similarly detected in the gas phase by ESI-MS (see ESI†).

Pleasingly, X-ray quality crystals of the complex adduct could be grown, an analysis confirming that the solid-state behaviour mirrors that of the solution-phase experiments (Fig. 5).‡ The cavitands interact *via* a cyclic seam of hydrogen bonds to give a pseudo-octagonal bipyramidal capsule with a volume of *ca.* 1500 Å^3 and dimensions of *ca.* 10.7 × 14.4 Å (excluding the alkyl feet, Fig. 5a and b). The internal cavity is 235 Å^3 of which 65% is occupied by the guest (152 Å^3), notably higher than the optimal 55% (ref. 43) (see ESI† for details of cavity and guest volume calculations).[44–46] This tight fit, combined with the rigid biconical topology of the cavity (Fig. 5d and e) forces the ethyl groups of the guest into magnetically anisotropic environments—*axial* (along the long axis of the capsule) and *equatorial* (in the plane of the cavitand rims)—resulting in the breaking of the guest's symmetry observed by NMR. The methyl groups of the axially-orientated substituents are buried deeply within the cavitand and localised over four aromatic rings, consistent with the large upfield shifts observed in the ^{1}H NMR spectrum. The phenolic protons of the host were well defined in the Fourier difference map and are positionally restrained only by their O···H distance (0.84 Å; Fig. 5c). The cavitands interact through seven intermolecular hydrogen-bonds (O···O distance 2.73–2.81 Å), six of which follow a head-to-tail arrangement around the capsule. Those groups not involved in cavitand–cavitand stabilization are free to form intramolecular hydrogen-bonds within the catechol subunit (*i.e.* O1···O2), or interact with MeOH solvent or the bromide counterion (Fig. 5c). In solution, these non-

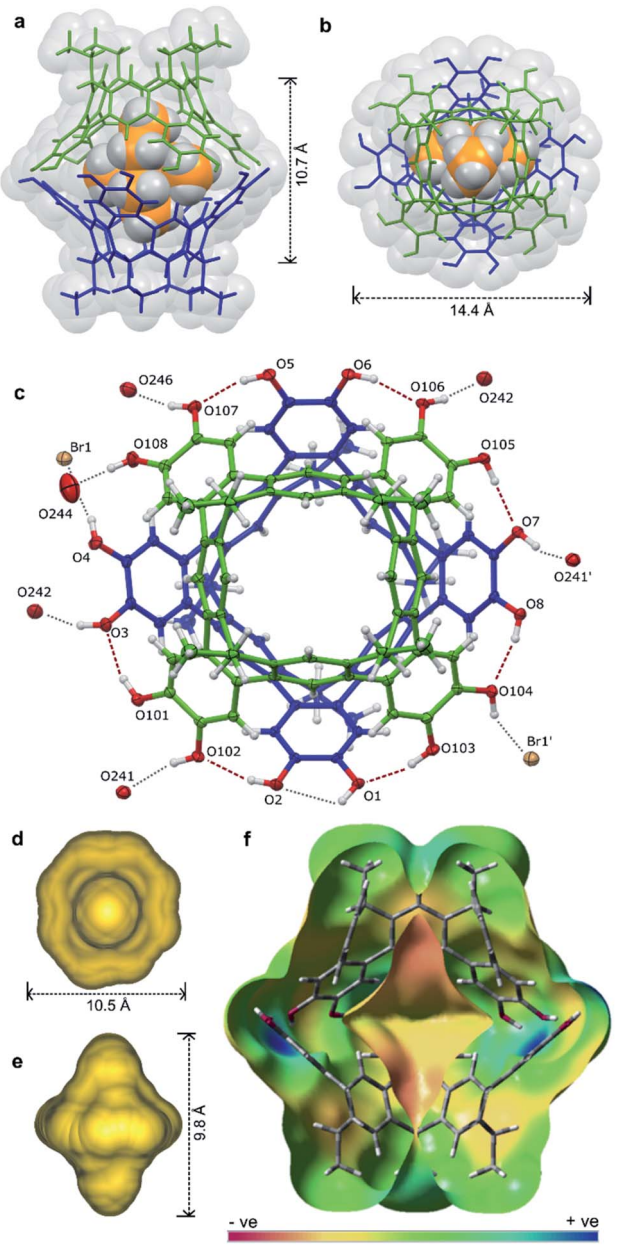

Fig. 5 The X-ray structure of [**2a**·**2a**⊂NEt_4]-Br·7.63MeOH·toluene·0.37$CHCl_3$ with guest, solvent and disorder omitted for clarity where necessary: the host guest complex (a) from the side and (b) top, (c) an ORTEP diagram showing the arrangement of hydrogen-bond donors and acceptors with the NEt_4^+ guest omitted for clarity, the calculated cavity surface (d) shown from the top and (e) side, and (f) a calculated electronic surface potential map of **2′**·**2′**, showing the electronegative surface of the cavity (see ESI† for details).

intermolecular hydrogen-bonds likely offer redundancy to the cavitand–cavitand interactions and may act to defend the dimer against interference by competitive media or bromide counterions.

The hydrogen-bonding motif is unprecedented for resorcin[4]arene-derived cavitands due to the coplanar arrangement of exoannuar hydroxyl groups, and may be thought of as an extension of the intercalated cyclotricatechylene (CTC)

"clamshell" dimers reported by Abrahams.[27] Here, the four catechol units of the interacting cavitands are rotationally offset by *ca.* 45° relative to the cavitand partner (compared to 60° for CTC dimers), the resulting greater cavity volume able to encapsulate larger guests with retention of the full hydrogen-bonding array.

An energy-optimised model of $\mathbf{2'\cdot 2'\subset CHCl_3}$ (B3LYP-D3/6-31G(d,p)) shows a cavity volume of 175 Å^3, 25% less than that measured experimentally with a bound NEt_4^+. As the monomer units are rigid, the volume difference arises through increased separation of the dimers (*ca.* +0.4 Å; measured between centroids calculated for O atoms of each cavitand) allowing the host to contract or expand at the hydrogen-bond equator to accommodate a range of guests with different volumes. Solution experiments support this analysis: the smaller guests NMe_4^+ (94 Å^3) and choline$^+$ (122 Å^3) are quantitatively sequestered despite volumes *ca.* 20–40% less than that of NEt_4^+. Notably, the complexes were stable in the polar solvent mixtures required to dissolve the salts (5% $CD_3OD/CDCl_3$), each evidencing slow exchange with the free guest (see ESI†). The ^{1}H NMR spectrum of $\mathbf{2b\cdot 2b\subset choline^+}$ shows only a single host species of S_8-symmetry, consistent with rapid tumbling of the guest on the NMR timescale at 298 K. The larger cation NPr_4^+ is not encapsulated, presumably due to the greater volume (227 Å^3) significantly disrupting the hydrogen-bonding array between interacting cavitands.

Neutral guests of a size and geometry complementary to the host cavity including adamantane (147 Å^3), $SiEt_4$ (176 Å^3) and terephthalonitrile (116 Å^3) showed no interaction, nor did the electron-poor aromatic C_6F_6 (113 Å^3). Calculated binding energies for the complexes $\mathbf{2'\cdot 2'\subset CHCl_3}$ and $\mathbf{2'\cdot 2'\subset SiEt_4}$ are indistinguishable within the range of error, whilst the cationic complexes $\mathbf{2'\cdot 2'\subset NEt_4^+}$ and $\mathbf{2'\cdot 2'\subset choline^+}$ enjoy significant stabilisation (Table 2; B3LYP-D3/6-311G++(2d,2p), *in vacuo*, see ESI† for full details). Electronic surface potential maps show the curvature of the host imparts a substantial electronegative bias to the internal surface of the cavity (Fig. 5f; see ESI†); it is likely that a favourable enthalpic contribution from π-basic···cation interactions drives the exchange of $CDCl_3$ for NEt_4^+, but not $SiEt_4$. The calculations show a strong energetic preference for NEt_4^+ over choline$^+$ (−33 kJ mol^{-1}; Table 2), behaviour replicated in solution as demonstrated by competition experiments between NMe_4^+, NEt_4^+ and choline$^+$. When 1 equivalent of each guest is combined together with the dimer host in 5% $CD_3OD/CDCl_3$, NMe_4^+ and NEt_4^+ are bound in a *ca.* 1 : 1.2 ratio, whereas the choline$^+$ complex is not detected (see ESI†). While the preference $NEt_4^+ \geq NMe_4^+ \gg$ choline$^+$ is difficult to reconcile based on the volume of the guests alone, it seems likely that the OH group of choline$^+$ interferes with the hydrogen-bonding motif between cavitands, destabilizing the complex. It should be noted that this geometry is not reflected in the calculated structure of the $\mathbf{2'\cdot 2'\subset choline^+}$ complex—possibly due to bias in the starting geometry—likely resulting in an overestimation of the binding energy.

Table 2 Calculated guest volumes and selected binding energies relative to $CHCl_3$ solvent

Guest	Guest vol. (Å^3)	$E_{binding}$[a] (kJ mol^{-1})
$CHCl_3$	71	0.0
NMe_4^+	94	−144
C_6F_6	113	—
Terephthalonitrile	116	—
Choline$^+$	122	−138
Adamantane	147	—
NEt_4^+	152	−171
$SiEt_4$	176	+2.1
NPr_4^+	227	—

[a] Relative energy of guest molecule displacing an encapsulated $CHCl_3$.

Conclusions

We have presented our observations into highly stable, self-assembled capsules stabilised by a cyclic seam of eight hydrogen bonds. The rigid cavity selectively sequesters and restricts the conformation of cationic guests, behaviour observed in both bulk solutions and the solid state, and analytically in the gas phase by ESI-MS. The hydrogen-bond array acts to articulate the interface between the rigid cavitands, allowing for some flexibility in the cavity volume and dimensions.

Data availability

All supporting data is provided in the ESI.†

Author contributions

N. T. L. conceived and supervised the project. J. N. S. carried out the experimental work and analyses, and C. E. performed the DFT calculations. J. N. S. drafted then refined the manuscript with input from C. E. and N. T. L.

Conflicts of interest

There are no conflicts to declare.

Acknowledgements

Financial support was provided by The MacDiarmid Institute for Advanced Materials and Nanotechnology, and the Marsden Fund Council, managed by the Royal Society Te Apārangi, New Zealand. J. N. S. thanks the University of Otago for the award of a PhD scholarship. C. E. thanks the National Computational Infrastructure (NCI: supported by the Australian Government) for high performance computing resources and services provided *via* project grant ay7.

Notes and references

‡ Crystal data for $\mathbf{2a\cdot 2a}\cdot C_8H_{20}N\cdot Br\cdot 7.63(CH_3OH)\cdot 0.37(CHCl_3)\cdot C_7H_8$: $C_{143}H_{154.89}BrCl_{1.11}NO_{23.63}$, $M = 2384.90$, pale-yellow block, 0.45 × 0.29 × 0.21 mm^3, triclinic, $a = 16.8535(2)$ Å, $b = 17.7481(2)$ Å, $c = 26.0471(4)$ Å, $\alpha = 82.9010(10)°$, $\beta = 71.9630(10)°$, $\gamma = 64.5340(16)°$, $V = 6688.07(16)$ Å^3, space group $P\bar{1}$ (#2), $Z = 2$,

μ(Mo-K$_\alpha$) = 0.397 mm^{-1}, $2\theta_{max}$ = 57.13°, $2\theta_{full}$ = 50.00° (99.7% complete), 128 545 reflections measured, 29 947 independent reflections (R_{int} = 0.0392). The final $R_1(F)$ = 0.0616 ($I > 2\sigma(I)$); 0.0824 (all data). The final w$R_2(F^2)$ = 0.1654 ($I > 2\sigma(I)$); 0.1815 (all data). GoF = 1.035.

1 L. J. Liu and J. Rebek, in *Hydrogen Bonded Supramolecular Structures*, ed. Z.-T. Li and L.-Z. Wu, Springer Berlin Heidelberg, Berlin, Heidelberg, 2015, pp. 227–248.
2 J. Kang and J. Rebek, *Nature*, 1997, **385**, 50–52.
3 Q. Zhang, L. Catti and K. Tiefenbacher, *Acc. Chem. Res.*, 2018, **51**, 2107–2114.
4 V. Angamuthu, M. Petroselli, F.-U. Rahman, Y. Yu and J. Rebek, *Org. Biomol. Chem.*, 2019, **17**, 5279–5282.
5 R. Wyler, J. de Mendoza and J. Rebek Jr, *Angew. Chem., Int. Ed. Engl.*, 1993, **32**, 1699–1701.
6 J. Kang and J. Rebek, *Nature*, 1996, **382**, 239–241.
7 L. R. MacGillivray and J. L. Atwood, *Nature*, 1997, **389**, 469.
8 T. Gerkensmeier, W. Iwanek, C. Agena, R. Fröhlich, S. Kotila, C. Näther and J. Mattay, *Eur. J. Org. Chem.*, 1999, **1999**, 2257–2262.
9 A. Shivanyuk and J. Rebek, *Chem. Commun.*, 2001, 2424–2425.
10 A. Shivanyuk and J. Rebek, *Proc. Natl. Acad. Sci. U. S. A.*, 2001, **98**, 7662.
11 L. Avram and Y. Cohen, *J. Am. Chem. Soc.*, 2002, **124**, 15148–15149.
12 L. Avram and Y. Cohen, *Org. Lett.*, 2002, **4**, 4365–4368.
13 L. Avram and Y. Cohen, *Org. Lett.*, 2003, **5**, 1099–1102.
14 L. Avram and Y. Cohen, *J. Am. Chem. Soc.*, 2004, **126**, 11556–11563.
15 K. Murayama and K. Aoki, *Chem. Commun.*, 1998, 607–608.
16 K. N. Rose, L. J. Barbour, G. W. Orr and J. L. Atwood, *Chem. Commun.*, 1998, 407–408.
17 A. Shivanyuk, E. F. Paulus and V. Böhmer, *Angew. Chem., Int. Ed.*, 1999, **38**, 2906–2909.
18 A. Shivanyuk, K. Rissanen and E. Kolehmainen, *Chem. Commun.*, 2000, 1107–1108.
19 A. Shivanyuk, E. F. Paulus, K. Rissanen, E. Kolehmainen and V. Böhmer, *Chem.–Eur. J.*, 2001, **7**, 1944–1951.
20 M. Luostarinen, A. Åhman, M. Nissinen and K. Rissanen, *Supramol. Chem.*, 2004, **16**, 505–512.
21 H. Mansikkamäki, C. A. Schalley, M. Nissinen and K. Rissanen, *New J. Chem.*, 2005, **29**, 116–127.
22 N. K. Beyeh and K. Rissanen, *Isr. J. Chem.*, 2011, **51**, 769–780.
23 A. Scarso, L. Pellizzaro, O. De Lucchi, A. Linden and F. Fabris, *Angew. Chem., Int. Ed.*, 2007, **46**, 4972–4975.
24 D. Beaudoin, F. Rominger and M. Mastalerz, *Angew. Chem., Int. Ed.*, 2016, **55**, 15599–15603.
25 B. C. Hamann, K. D. Shimizu and J. Rebek, *Angew. Chem., Int. Ed. Engl.*, 1996, **35**, 1326–1329.
26 E. Huerta, G. A. Metselaar, A. Fragoso, E. Santos, C. Bo and J. de Mendoza, *Angew. Chem., Int. Ed.*, 2007, **46**, 202–205.
27 B. F. Abrahams, N. J. FitzGerald, T. A. Hudson, R. Robson and T. Waters, *Angew. Chem., Int. Ed.*, 2009, **48**, 3129–3132.
28 D. J. Cram, S. Karbach, Y. H. Kim, L. Baczynskyj, K. Marti, R. M. Sampson and G. W. Kalleymeyn, *J. Am. Chem. Soc.*, 1988, **110**, 2554–2560.
29 T. Gerkensmeier, J. Mattay and C. Näther, *Chem.–Eur. J.*, 2001, **7**, 465–474.
30 A. Shivanyuk and J. J. Rebek, *Chem. Commun.*, 2001, 2374–2375.
31 M. C. Letzel, B. Decker, A. B. Rozhenko, W. W. Schoeller and J. Mattay, *J. Am. Chem. Soc.*, 2004, **126**, 9669–9674.
32 Y. S. Park and K. Paek, *Org. Lett.*, 2008, **10**, 4867–4870.
33 C. B. Aakeröy, A. Rajbanshi and J. Desper, *Chem. Commun.*, 2011, **47**, 11411–11413.
34 T. Heinz, D. M. Rudkevich and J. Rebek, *Nature*, 1998, **394**, 764–766.
35 M. H. K. Ebbing, M.-J. Villa, J.-M. Valpuesta, P. Prados and J. de Mendoza, *Proc. Natl. Acad. Sci. U. S. A.*, 2002, **99**, 4962–4966.
36 J. N. Smith and N. T. Lucas, *Chem. Commun.*, 2018, **54**, 4716–4719.
37 J. N. Smith, T. K. Brind, S. B. Petrie, M. S. Grant and N. T. Lucas, *J. Org. Chem.*, 2020, **85**, 4574–4580.
38 L. Avram and Y. Cohen, *Chem. Soc. Rev.*, 2015, **44**, 586–602.
39 T. Szabo, G. Hilmersson and J. Rebek, *J. Am. Chem. Soc.*, 1998, **120**, 6193–6194.
40 D. B. Hibbert and P. Thordarson, *Chem. Commun.*, 2016, **52**, 12792–12805.
41 K. J. Winstanley, A. M. Sayer and D. K. Smith, *Org. Biomol. Chem.*, 2006, **4**, 1760–1767.
42 M. Chwastek, P. Cmoch and A. Szumna, *Angew. Chem., Int. Ed.*, 2021, **60**, 4540–4544.
43 J. Rebek, *Acc. Chem. Res.*, 1999, **32**, 278–286.
44 A. Pedretti, L. Villa and G. Vistoli, *J. Mol. Graphics Modell.*, 2002, **21**, 47–49.
45 A. Pedretti, L. Villa and G. Vistoli, *J. Comput.-Aided Mol. Des.*, 2004, **18**, 167–173.
46 A. Jurcik, D. Bednar, J. Byska, S. M. Marques, K. Furmanova, L. Daniel, P. Kokkonen, J. Brezovsky, O. Strnad, J. Stourac, A. Pavelka, M. Manak, J. Damborsky and B. Kozlikova, *Bioinformatics*, 2018, **34**, 3586–3588.